JOURNAL OF SOLID STATE CHEMISTRY **127,** 56–63 (1996)
ARTICLE NO. 0356

A Neutron Diffraction Study of Ca Doped and Oxygen Deficient $YBa_2Cu_3O_{7-\delta}$

P. Berastegui*,[1] S.-G. Eriksson,* L.G. Johansson,* M. Kakihana,† M. Osada,† H. Mazaki,‡ and S. Tochihara‡

*Department of Inorganic Chemistry, Chalmers University of Technology and University of Göteborg, S-412 96 Göteborg, Sweden; †Materials and Structures Laboratory, Tokyo Institute of Technology, Nagatsuta 4259, Midori-ku, Yokohama 226, Japan; and ‡Department of Mathematics and Physics, The National Defense Academy, Yokosuka 239, Japan

Received May 20, 1996; in revised form August 5, 1996; accepted August 8, 1996

A detailed study of the structure of Ca doped $YBa_2Cu_3O_{7-\delta}$ samples with different oxygen contents has been carried out. Neutron powder diffraction data were collected for nine samples with varying Ca and oxygen contents and the structural changes were determined by Rietveld refinement. The samples were prepared by annealing at different oxygen partial pressures and for the undoped samples δ values of 0.03, 0.38, and 0.95 were obtained. A decrease in the oxygen content with Ca doping is observed for the orthorhombic samples. T_c decreases due to overdoping in the fully oxidized samples and increases in the partially oxidized samples. The bond lengths change in a similar manner for both the fully and partially oxidized samples. The structural changes are related to the increasing oxygen deficiency in the CuO chains and to the change in average charge and ion size at the Y site. In the fully reduced samples, only the oxygen ions at the CuO_2 planes are significantly affected by substitution.

1. INTRODUCTION

Attempts to increase the superconducting transition temperature in $YBa_2Cu_3O_{7-\delta}$ (Y-123), cf. Fig. 1, by means of nonisovalent substitutions demonstrated that the structure responds to the substitution by compensating the charge difference with a change of the oxygen content (1, 2). Ca doping at the Y site and La doping at the Ba site thus decreases and increases the oxygen content, respectively, resulting in a degradation of the superconducting properties. Interestingly, Ca substitution in $Y_{1-x}Ca_xBa_2Cu_3O_{7-\delta}$ changes the oxygen content according to the relation $\delta \approx \delta_0 + x/2$ which would have the consequence of keeping the average oxidation state of Cu constant. However, this ratio is highly dependent on the annealing procedure (3). The structural effects of a lowering of the oxygen content have been characterized in detail in Refs. (4, 5). A charge transfer mechanism that depletes the superconducting CuO_2 planes of charge carriers by transferring holes from the CuO_2 planes to the CuO chains where they are localized has been established as the cause of the depression of T_c. The structural changes occurring upon Ca substitution have also been studied previously in oxidized samples (6), in oxygen depleted samples (7), and recently in oxygen deficient samples (8). In the first case, the atomic displacements and the decrease in T_c can be related to the effects of the variation in oxygen content. Therefore, the additional hole content provided by Ca substitution is thought to be reduced by the induced oxygen depletion. On the other hand, the tetragonal phase becomes superconducting at doping levels of $x \geq 0.2$ due to the increase of the charge carrier content. Superconductivity can thus be restored in the insulating $YBa_2Cu_3O_6$ and in $PrBa_2Cu_3O_7$ by the same mechanism (9, 10). Casalta *et al.* (9) have determined the phase diagram of the $Y_{1-x}Ca_xBa_2Cu_3O_6$ system, where an antiferromagnetic phase is observed for $x < 0.07$ and the superconducting phase for $x \geq 0.2$. Like most cuprate superconducting materials, Y-123 exhibits a parabolic dependence of T_c upon the charge carrier concentration (11) and the fully oxygenated $YBa_2Cu_3O_7$ is considered to be slightly overdoped (12). Thus, further hole doping would decrease T_c as in the $La_{1-x}Sr_xCuO_4$ compound (13).

The electrical transport properties and the carrier density have been studied thoroughly by measurements of the Hall coefficient (14–17), thermoelectric power (18, 19), NMR (9, 20), and NQR (21). Studies of the resistivity behavior in $Y_{0.8}Ca_{0.2}Ba_2Cu_3O_{7-\delta}$ samples showed that the resistivity at room temperature increases with δ and that it is affected by the annealing procedure (14). These observations suggested that the charge reservoir role of the CuO chains is strongly affected by Ca doping. NMR measurements have shown that in oxidized samples, the introduction of holes at the CuO_2 planes by Ca doping is compensated by the induced oxygen vacancies and that the compounds are overdoped (20). NQR studies on reduced

[1] To whom all correspondence should be addressed.

0022-4596/96 $18.00

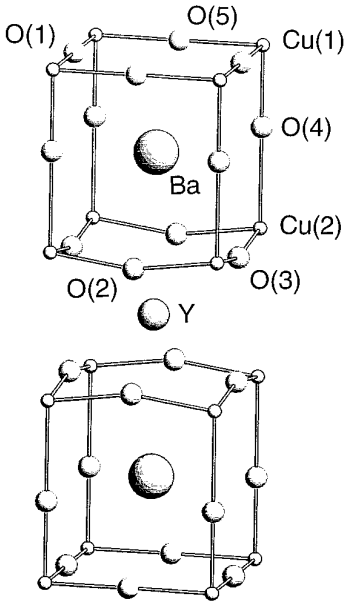

FIG. 1. Unit cell of $YBa_2Cu_3O_7$ illustrating the nomenclature used in the text. The oxygen site O(5) is only partially occupied.

samples showed that the CuO chains are not affected by hole doping through Ca substitution and that the holes generated at the CuO_2 planes destroy the antiferromagnetic ordering and induce superconductivity (21).

In this study, we present a detailed characterization of the structural changes that occur in $YBa_2Cu_3O_{7-\delta}$ samples with Ca substitution where, for the undoped samples, $7-\delta \approx 6.97, 6.62, 6.05$.

2. EXPERIMENTAL

A series of polycrystalline samples with stoichiometry $Y_{1-x}Ca_xBa_2Cu_3O_{7-\delta}$, $0 \le x \le 0.3$, was prepared by solid state reaction of Y_2O_3, $CaCO_3$, $BaCO_3$, and CuO powders which were mixed and ground in ethanol before firing. The samples were sintered first as powders at 900°C in air for 24 h, ground and pelletized, and then sintered at 930°C for 48 h in air. Two more sinterings were carried out at 950°C for 60–80 h in an oxygen atmosphere to obtain well-crystallized samples. No impurities, such as $BaCuO_2$, could be detected by X-ray diffraction analyses using the Guinier film technique in samples with $x \le 0.20$. Annealing was performed at 400°C in an oxygen atmosphere for a period of two days or longer. At this point, each sample was divided into three parts and annealings were carried out following the work of Jorgensen *et al.* (4). To prepare partially oxidized samples with an oxygen content close to 6.6 for the undoped Y-123 sample, the following procedure was used. The samples were heated to 900°C in air and cooled to 520°C at a rate of 180°C/h, at which temperature annealing in 2% O_2 in Ar was performed for three days with a gas flow of approximately 0.5 liter/min before quenching into liquid nitrogen. Fully reduced samples were prepared by a similar procedure but were annealed at 640°C in pure argon instead. X-ray diffraction analyses revealed a tetragonal unit cell for the latter samples and showed that no impurities such as green phase (Y_2BaCuO_5) had formed during the annealings. Iodometric titration was used to obtain an independent determination of the oxygen content. A decreasing oxygen content could be observed with Ca doping except for in the fully reduced samples, where a nearly constant oxygen content around 6.03(2) was found. To correctly establish the effects of Ca doping on T_c, a comparison was made between a sample with the stoichiometry $Y_{0.9}Ca_{0.1}Ba_2Cu_3O_{6.5}$ and a sample with $x = 0.2$ and an oxygen content of 6.5 as determined from iodometric titration. The latter sample was prepared by annealing in a 10% O_2 in Ar gas mixture at 520°C. In the following discussion, the three series of samples will be referred to as series A (fully oxidized), B (partially oxidized), and C (fully reduced).

Neutron diffraction experiments were carried out at the spallation source ISIS, RAL, using the high flux, medium resolution diffractometer POLARIS. At this diffractometer, the detectors at back scattering cover a d range of 0.2–3.2 Å with a resolution of $\Delta d/d \approx 5 \times 10^{-3}$. Time-of-flight data were collected for the nine samples with volumes of 3–3.5 cm^3 at room temperature. After focusing and normalization, refinements were made with TF15LS (22), a Rietveld program especially developed for least-squares refinement of time-of-flight data. The scattering lengths used were taken from Ref. (23). The refinements were carried out assuming that Ca substitution occurred only at the Y site and that the O(5) site at the (1/2,0,0) position was partially occupied. Due to the low occupancies obtained at this site in the orthorhombic samples and at the O(1) site at (0, 1/2, 0) in the tetragonal samples, their isotropic temperature factors were fixed at 0.5 $Å^2$. Anisotropic temperature factors were refined for the O(1) and O(4) atoms but as it did not result in an improvement of the description of the thermal motion or the reliability values, all atoms were refined with isotropic temperature factors. At the last steps of the refinement, the occupancies for the other atoms were allowed to vary, but it resulted in full occupancies within e.s.d.'s. The nominal stoichiometry also agreed well with the refined Ca occupancy at the Y site. Figure 2 shows a relevant part of the diffraction pattern (raw data) for the samples under study. The transition to a tetragonal symmetry can be observed with decreasing oxygen content. In Table 1, the structural parameters for the samples under study are presented together with the superconducting transition temperatures which were measured in terms of the complex ac

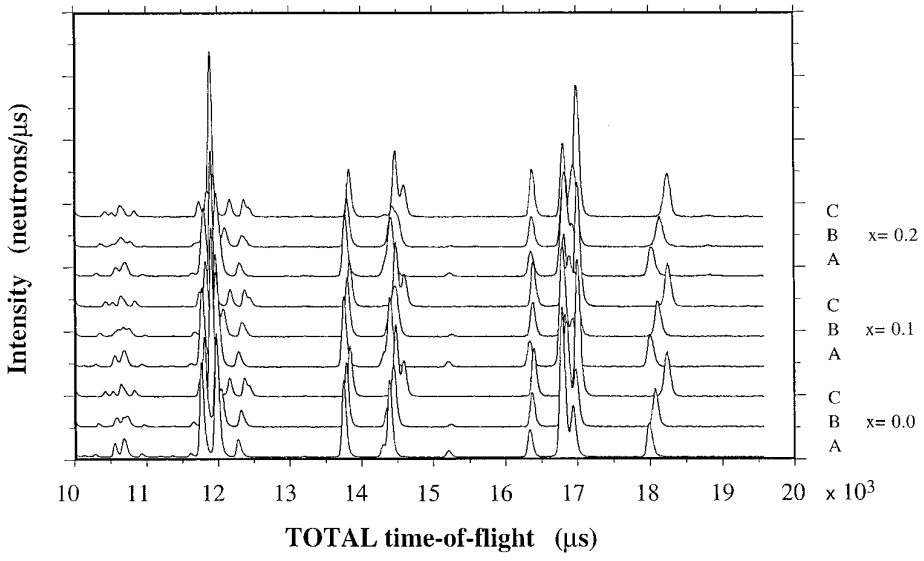

FIG. 2. Part of the neutron diffraction patterns collected for the $Y_{1-x}Ca_xBa_2Cu_3O_{7-\delta}$ samples, including fully oxidized (series A), partially oxidized (series B), and fully reduced samples (series C).

susceptibility with a frequency of 132 Hz and amplitude of 100 mOe. The $YBa_2Cu_3O_{6.04}$ sample was nonsuperconducting while, with 10% Ca doping, the fully reduced sample became superconducting at $T_{c,onset}$ = 19.8 K. However, the volume fraction of the superconducting bulk phase was relatively small in this sample. T_c was also observed to increase in the partially oxidized samples, while it decreased in the fully oxidized samples.

TABLE 1
T_c Values and Structural Parameters for Oxygen Deficient Samples of $Y_{1-x}Ca_xBa_2Cu_3O_{7-\delta}$

Series		A			B			C		
x		0.0	0.1	0.2	0.0	0.1	0.2	0.0	0.1	0.2
$T_{c,onset}$ (K)		90.1	85.2	80.9	63.1	79.3	77.5	—	19.8	43.5
a (Å)		3.8141(1)	3.8169(1)	3.8249(1)	3.8275(1)	3.8340(1)	3.8393(1)	3.8588(1)	3.8569(1)	3.8540(1)
b (Å)		3.8806(1)	3.8777(1)	3.8791(1)	3.8814(1)	3.8781(1)	3.8680(1)	$=a$	$=a$	$=a$
c (Å)		11.6702(1)	11.6788(1)	11.6928(1)	11.7231(1)	11.7454(1)	11.7637(1)	11.8269(1)	11.8354(1)	11.8298(1)
V (Å^3)		172.73(1)	172.86(1)	173.49(1)	174.16(1)	174.64(1)	174.70(1)	176.11(1)	176.06(1)	175.71(1)
Y/Ca	B (Å^2)	0.24(1)	0.24(1)	0.27(1)	0.28(1)	0.32(1)	0.38(1)	0.34(1)	0.34(1)	0.36(1)
Ba	z	0.18374(8)	0.18476(9)	0.1862(1)	0.18775(8)	0.18918(8)	0.19099(9)	0.19472(7)	0.19524(7)	0.19526(8)
	B (Å^2)	0.40(1)	0.42(1)	0.46(1)	0.42(1)	0.47(1)	0.51(2)	0.46(1)	0.47(1)	0.50(1)
Cu(1)	B (Å^2)	0.20(1)	0.30(1)	0.44(1)	0.39(1)	0.51(1)	0.62(2)	0.64(1)	0.72(1)	0.79(1)
Cu(2)	z	0.35477(5)	0.35545(5)	0.35464(6)	0.35677(5)	0.35771(6)	0.35893(7)	0.36080(5)	0.36104(5)	0.36113(5)
	B (Å^2	0.29(1)	0.29(1)	0.28(1)	0.28(1)	0.28(1)	0.26(1)	0.24(1)	0.25(1)	0.24(1)
O(1)	B (Å^2)	0.72(3)	0.80(3)	0.86(5)	0.84(5)	1.05(7)	1.5(1)	0.5	0.5	0.5
	n	0.94(1)	0.89(1)	0.79(1)	0.61(1)	0.53(1)	0.43(1)	0.05(1)	0.04(1)	0.04(1)
O(2)	z	0.37846(8)	0.3776(1)	0.3766(1)	0.3788(1)	0.3779(1)	0.3784(2)	0.37909(5)	0.37829(5)	0.37743(5)
	B (Å^2)	0.44(1)	0.47(1)	0.48(2)	0.43(1)	0.48(2)	0.47(2)	0.44(1)	0.47(1)	0.50(1)
O(3)	z	0.37843(9)	0.3777(1)	0.3768(1)	0.3783(1)	0.3776(1)	0.3758(2)			
	B (Å^2)	0.42(1)	0.41(1)	0.41(2)	0.42(2)	0.43(2)	0.45(3)			
O(4)	z	0.15873(7)	0.15819(8)	0.1575(1)	0.15647(8)	0.15563(9)	0.1542(1)	0.15263(9)	0.15220(9)	0.1519(1)
	B (Å^2)	0.50(1)	0.60(1)	0.78(2)	0.70(1)	0.86(2)	1.13(2)	0.89(1)	0.97(1)	1.09(2)
O(5)	n	0.03(1)	0.03(1)	0.04(1)	0.01(1)	0.02(1)	0.06(1)			
$7-\delta$		6.97	6.92	6.83	6.62	6.55	6.49	6.05	6.04	6.04
R_p		3.2	3.3	3.6	3.6	3.4	3.5	3.4	3.0	3.6
R_{wp}		2.2	2.2	2.5	2.3	2.3	2.7	2.5	2.4	2.7
χ^2		6.3	6.7	9.9	7.8	8.0	9.1	9.9	7.0	8.6
R_I		2.7	2.3	2.5	3.4	2.8	3.3	4.2	3.5	3.5

Note. Space groups *Pmmm* (No. 47) and *P*4/*mmm* (No. 123). Y at (1/2, 1/2, 1/2), Ba at (1/2, 1/2, z), Cu(1) at (0, 0, 0), Cu(2) and O(4) at (0, 0, z), O(1) at (0, 1/2, 0), O(2) at (1/2, 0, z), O(3) at (0, 1/2, z), O(5) at (1/2, 0, 0)

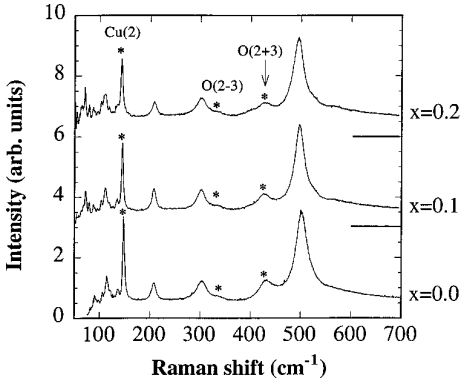

FIG. 3. Unpolarized micro-Raman spectra of the fully oxidized $Y_{1-x}Ca_xBa_2Cu_3O_{7-\delta}$ samples recorded at room temperature. The lines denote the zero intensity levels for the spectrum immediately above. The CuO_2 plane phonons are marked by asterisks (*) together with mode assignments using simple atomic notations.

3. DISCUSSION

The annealing procedure greatly influences the degree of oxidation of Ca doped $YBa_2Cu_3O_{7-\delta}$ samples. Thus, annealing periods of 1 or 2 days resulted in an incomplete oxidation. Annealing at 400°C and 60 atm of oxygen pressure for 2 days was sufficient to fully oxidize the materials, but the oxygen content did not increase over the one obtained by annealing the samples for 3 to 7 days at 1 atm oxygen pressure. T_c is reduced with increasing Ca content in the fully oxygenated samples at a rate of 5 K per 10% Ca at the Y site (see Table 1). It was also observed that $T_{c,onset}$ increased from 79.3 K in $Y_{0.9}Ca_{0.1}Ba_2Cu_3O_{6.5}$ to 84.8 K in $Y_{0.8}Ca_{0.2}Ba_2Cu_3O_{6.5}$, the oxygen contents in these samples being determined from iodometric titration. Thus, it is clear that Ca substitution in samples with a constant oxygen content increases T_c. Assuming that the compounds are underdoped, the substitution of Ca for Y would dope the CuO_2 planes with holes and increase T_c as observed for these two samples.

Further understanding of the doping process in $Y_{1-x}Ca_xBa_2Cu_3O_{7-\delta}$ is obtained from the change in the optical phonons. Figure 3 shows unpolarized micro-Raman spectra of the fully oxidized samples recorded at room temperature. Here, we focus on three CuO_2 plane phonons (at 145, 340, and 440 cm^{-1}), as they concern atoms directly involved in the superconductivity. Details for all other Raman modes in the $Y_{1-x}Ca_xBa_2Cu_3O_{7-\delta}$ system will be presented in a separate publication. When the Ca content increases, all these CuO_2 plane phonons decrease in intensity. The same behaviors are also observed in both the partially oxidized and fully reduced samples, and therefore they are characteristic for the Ca doping in all the $Y_{1-x}Ca_xBa_2Cu_3O_{7-\delta}$ series. These effects are most probably direct manifestations of the increase in the number of charge carriers induced by Ca doping. Similar effects have also been observed for the corresponding vibrations related to the CuO_2 planes in $Bi_2Sr_2Y_{1-x}Ca_xCu_2O_{8+\delta}$ with increasing Ca doping (24).

The increase in the hole concentration at the CuO_2 planes with Ca doping can also be estimated using bond valence sums (BVS). In a recent work, the dependence of T_c and thermoelectric power upon hole content in $Y_{1-x}Ca_xBa_2Cu_3O_{7-\delta}$ samples has been shown to follow the same trend as in other superconducting systems (25). We have calculated the BVS around the Cu(2) ion in the CuO_2 planes from our structural data using a model that takes into account the presence of Cu^{3+} (26, 27). Furthermore, the two parameters suggested by J. L. Tallon were used to properly correlate T_c with the bond valence sums around the ions at the CuO_2 planes (28). These two variables are the difference and the sum of the Cu and O bond valence sums and while the former ($V_- = 2 + V_{Cu(2)} - V_{O(2)} - V_{O(3)}$) describes the hole density in the CuO_2 planes, the latter ($V_+ = 6 - V_{Cu(2)} - V_{O(2)} - V_{O(3)}$) describes the preference for the distribution of holes on oxygen sites relative to copper sites. The parameter V_+ was found to remain relatively constant as in the case of $YBa_2Cu_3O_{7-\delta}$ (28), at a value of -0.26 ± 0.04, indicating a constant preference for the distribution of holes on oxygen sites. Figure 4 shows the plot of V_- versus T_c in the Ca doped 123 samples studied in this work together with the values calculated from the structural data for $YBa_2Cu_3O_{7-\delta}$ samples reported by Cava *et al.* (5). It can be observed that T_c increases up to a maximum at a hole density of about 0.2 holes per Cu in the CuO_2 planes, and then decreases due to overdoping of the CuO_2 planes in the fully oxidized samples. The oxygen depletion that is observed with Ca

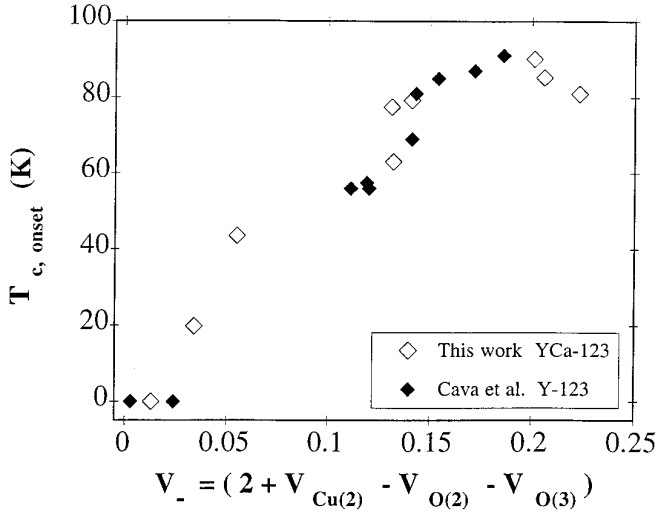

FIG. 4. T_c values in Ca doped 123 samples as a function of the hole density on the CuO_2 planes, V_-(◇). As a comparison, the values calculated from Ref. (5) for $YBa_2Cu_3O_{7-\delta}$ samples are also included (◆).

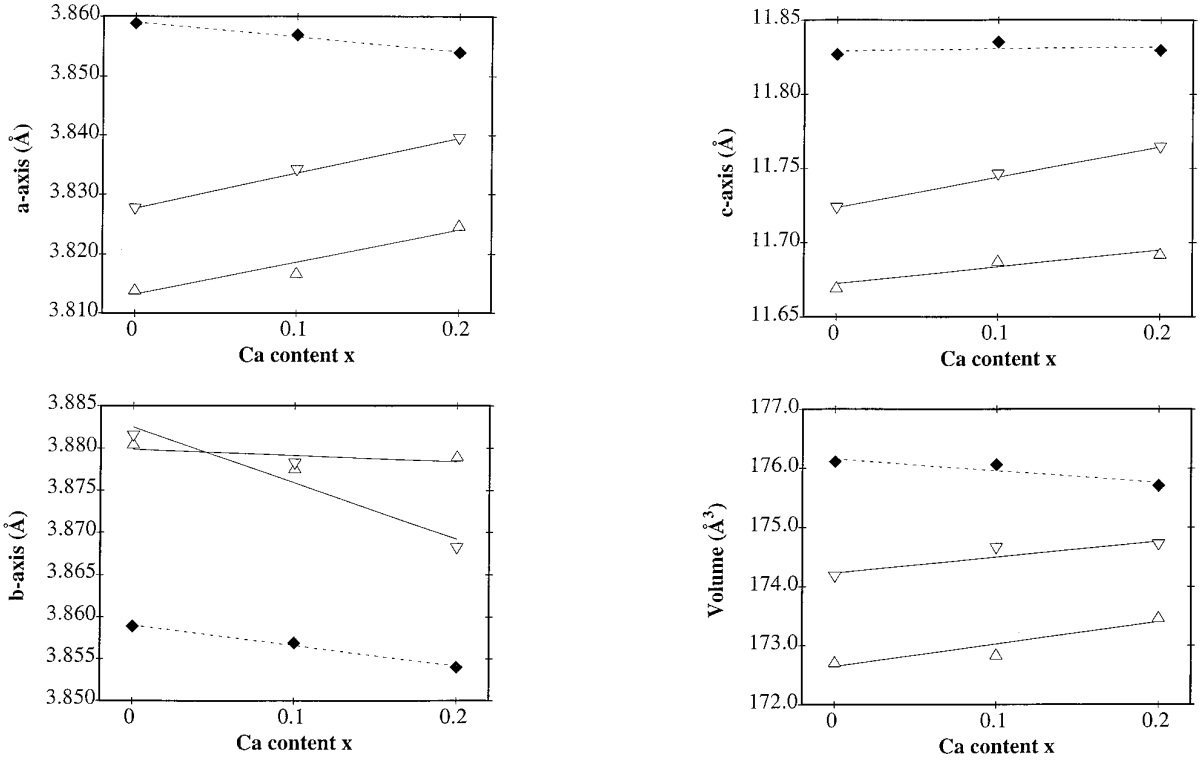

FIG. 5. Changes in cell parameters and unit cell volume in $Y_{1-x}Ca_xBa_2Cu_3O_{7-\delta}$ samples [series A (△), series B (▽), series C (♦)].

doping implies that the average oxidation state of copper remains nearly constant. Therefore, the reduced positive charge at the Y site can be considered to induce a redistribution of holes between the CuO chains and the CuO_2 planes that causes an increase of the hole content at the planes. Moreover, it has been reported that the disappearance of T_c in Ca doped Y-123 samples occurs at higher δ values than in oxygen deficient Y-123 samples. This would imply that the carriers provided by Ca doping are not completely compensated by the induced oxygen vacancies and cause the overdoping of the CuO_2 planes at high oxygen contents (14).

In the fully reduced samples, the appearance of superconductivity is observed at $x = 0.1$, in contrast to previous reports of values around $x = 0.2$; see, e.g., Ref. (9). Thus, a small increase of the hole density at the planes induces superconductivity in this system. The disagreement with the previous work on the effect on T_c of Ca doping in $YBa_2Cu_3O_6$ may be due to differences in the sintering and annealing procedure and to the fact that our samples were quenched. The partially oxidized samples are considered to be well underdoped and Ca substitution results in the doping of the CuO_2 planes with holes which increases T_c. Furthermore, a T_c plateau has been observed in this system at oxygen contents close to those determined for the samples in this series and the rapid increase and thereafter nearly constant T_c values observed in this series (B) may be due to such an effect. A similar increase of T_c has been observed by Awana *et al.* (8) and Kontos *et al.* (20). In the latter work, the temperature dependence of the Knight shift suggested that the partially oxidized samples were underdoped while fully oxygenated samples were overdoped. The creation of holes due to Ca doping would thus cause an increase and a decrease in T_c in the two series of samples, respectively.

The larger size of Ca^{2+} ($r = 1.12$ Å) compared to Y^{3+} ($r = 1.019$ Å) is expected to cause an expansion around the Y site in all three series of samples, but considering the induced oxygen depletion, such a correlation is expected to be more obvious in the fully reduced samples. In this case however, a decrease of the *a* and *b* axes and of the unit cell volume is observed, the *c* axis remaining nearly constant. Figure 5 shows the changes in cell parameters and unit cell volume as determined from the neutron diffraction data. The decrease of the orthorhombicity is nearly twice as large for the samples with lower oxygen content (series B). This behavior is dependent mainly on the shortening of the *b* axis, as the orthorhombicity decreases more rapidly close to the transition from orthorhombic to tetragonal symmetry at values of $\delta \approx 0.65$ (4).

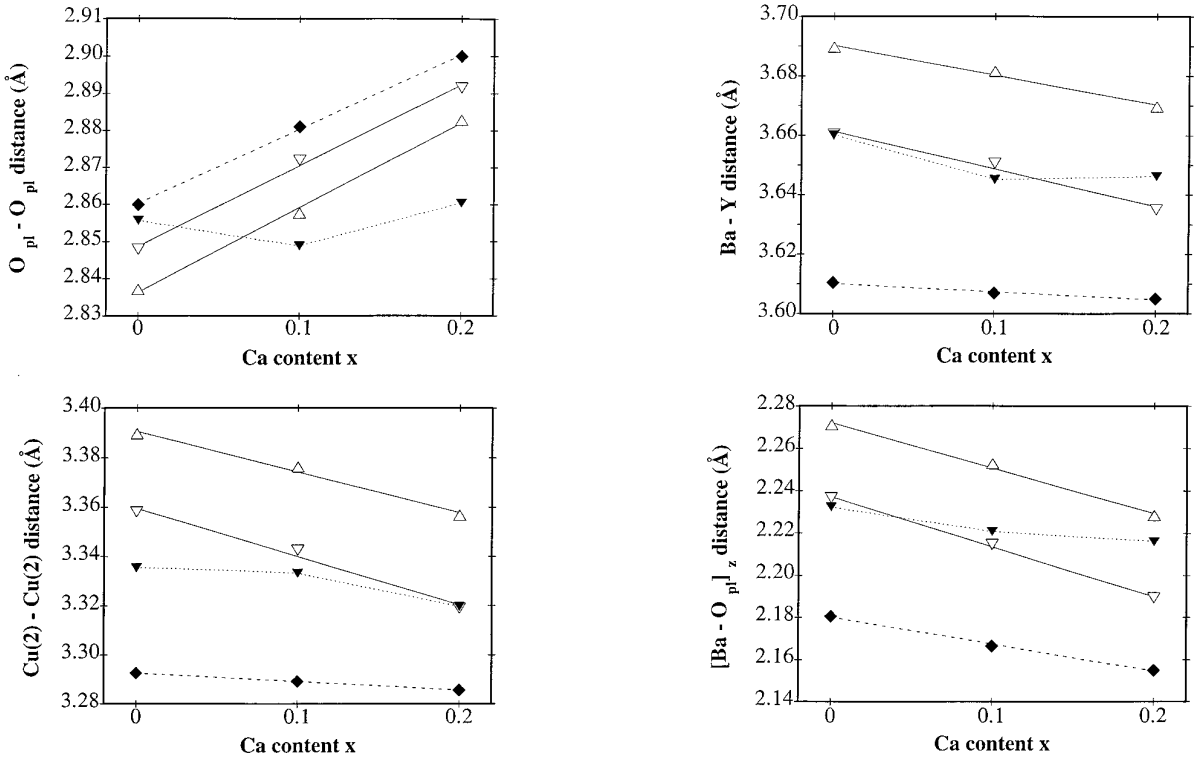

FIG. 6. Bond length changes around the Y and Ba sites in $Y_{1-x}Ca_xBa_2Cu_3O_{7-\delta}$ samples [series A (△), series B (▽), series C (◆)]. The data from the work of Jorgensen *et al.* (4) on $YBa_2Cu_3O_{7-\delta}$ has been included as a comparison (▼). Error bars are smaller than the symbols.

Figure 6 shows that the bond length changes around the Y site. The increase of the O_{plane}–O_{plane} distance and the decrease of the Cu(2)–Cu(2) distance along the *c* axis are expected to be partly due to the introduction of Ca at the Y site. Jorgensen *et al.* (4) reported on the structural changes that occur in Y-123 as a function of the oxygen deficiency and include samples with $\delta = 0.40$, 0.45, and 0.52 in their investigation. These compositions are close to those studied in series B in this work and a comparison showed that with increasing oxygen deficiency, the observed bond length changes are more marked in Ca doped samples than in undoped samples. Considering, e.g., the O_{pl}–O_{pl} distance, the observed increase in the three series is due to the introduction of Ca at the Y site, as this distance increases only slightly for $0 < \delta < 1$ in the undoped samples (4). Thus, although the changes observed for the orthorhombic samples are mainly caused by the oxygen deficiency, an additional contribution is due to the lower positive charge at the Y site, as has been discussed for cosubstituted Y-123 samples, e.g., $Y_{1-x}Ca_xBa_2Cu_{2.7}Co_{0.3}O_{7-\delta}$ (29, 30). These trends for the O_{pl}–O_{pl} and Cu(2)–Cu(2) distances have also been observed in Ca doped Y-124 samples where the oxygen content is constant (31).

The puckering of the CuO_2 planes decreases with Ca doping for all three series of samples indicating that it has no direct relation to the suppression or appearance of superconductivity in this system. Moreover, the CuO_2 planes are flattened at a faster rate in Ca doped samples than in undoped samples due to the lower charge at the Y site in the former samples. It can also be observed that the Cu(2)–Cu(2) distance remains constant with Ca doping in the tetragonal samples. Thus, the Cu(2)–Cu(2) distance is associated with the transfer of charge between the planes and the chains, as there is no clear evidence of such an effect taking place in this series. Therefore, in the tetragonal samples, the Cu(2)–Cu(2) distance remains constant due to the absence of charge transfer, and the O_{pl}–O_{pl} distance increases due to the charge and size of the Ca ion.

Figure 6 also illustrates the changes in bond lengths along the *c* axis that could be associated with the nonisovalent substitution, i.e., the Ba–Y and $[Ba–O_{pl}]_z$ distances. With the decrease in charge at the Y site and oxygen depletion, the Ba ion is expected to be displaced toward the CuO_2 planes, which is indeed observed. However, the main reason for this displacement seems to be the depletion of oxygen from the single chains, as the decrease of the Ba–Y distance is not so significant in the tetragonal samples. Thus, while the planes are mainly affected by Ca doping, the chains are to a large extent only affected by the reduced oxygen content. The latter effect can be deduced from the Cu(2)–Cu(1) distance that remains unaffected in the tetragonal samples.

Charge transfer has been established in the case of a decrease of the oxygen content in Y-123. The bond lengths related to this model concern the apical oxygen that moves away from the CuO_2 planes as T_c decreases; see Fig. 7. The same changes are observed for the Ca doped series although less markedly in the tetragonal samples which would indicate that the holes that are introduced at the Y site with Ca substitution remain at the CuO_2 planes. Furthermore, in the tetragonal samples, the $[Ba–O(4)]_z$ distance, which is an indicator of charge transfer, was also found to remain unaffected by the substitution.

The structural changes lead to several conclusions. First, Ca substitution has a large influence on the oxidation and reduction processes that take place during annealing and doping. Second, the appearance of superconductivity in the tetragonal samples is not reflected in any anomalies in the trends observed for the bond lengths. Moreover, the trends in the structural changes do not directly reflect the degree of oxidation of the CuO_2 planes. Third, the reduced positive charge at the Y site induces a redistribution of holes between the CuO chains and the CuO_2 planes. Ca doping increases the hole content at the CuO_2 planes which leads to a decrease of T_c in overdoped samples and an increase of T_c in underdoped samples. Finally, the structural trends observed in the orthorhombic samples are a combination of the effects of Ca doping and oxygen depletion, while in the tetragonal samples, the effects of Ca doping predominate.

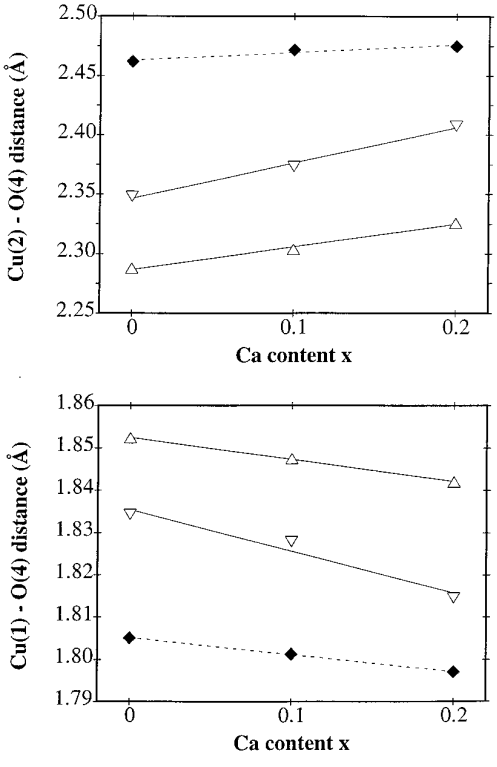

FIG. 7. Bond distances to the apical oxygen in $Y_{1-x}Ca_xBa_2Cu_3O_{7-\delta}$ samples [series A (△), series B (▽), series C (◆)]. Error bars are smaller than the symbols.

4. SUMMARY

We have presented a study of the structural changes occurring upon substitution of Ca for Y in a series of $YBa_2Cu_3O_{7-\delta}$ samples with different oxygen contents. A decrease of the oxygen content was observed with increasing Ca substitution in orthorhombic samples. The decrease of T_c in fully oxidized samples can be associated to overdoping and the structural changes mainly to the induced oxygen depletion at the single chains. At lower oxygen contents, the substitution of Ca in orthorhombic samples causes an increase in T_c that is related to the compounds being underdoped. The changes in cell parameters for these samples were found to follow the same trends and reflect the oxygen depletion at the CuO chains and the lowered charge at the Y site. In the tetragonal samples, superconductivity appears at a Ca content about $x = 0.1$. The oxygen content remained constant in these samples and no significant charge transfer was indicated by the structural changes.

ACKNOWLEDGMENTS

We are grateful to Dr. S. Hull and Dr. R. Smith, ISIS, RAL, for their assistance during the neutron diffraction experiments and to Dr. C. Ström for applying for the beam time needed to carry out the data collection. The Swedish Natural Science Research Council is acknowledged for financial support. M.O. acknowledges the financial support of The Japan Society for The Promotion of Science. This work is partially supported by Grant-in-Aid for Scientific Research 08455012 and 4482 from The Ministry of Education, Science, and Culture of Japan.

REFERENCES

1. Y. Tokura, J. B. Torrance, T. C. Huang, and A. I. Nazzal, *Phys. Rev. B* **38,** 7156 (1988).
2. A. Manthiram, S.-J. Lee, and J. B. Goodenough, *J. Solid State Chem.* **73,** 278 (1988).
3. A. Tokiwa, Y. Syono, M. Kikuchi, R. Suzuki, T. Kajitani, N. Kobayashi, T. Sasaki, O. Nakatsu, and Y. Muto, *Jpn. J. Appl. Phys.* **27,** L1009 (1988).
4. J. D. Jorgensen, B. W. Veal, A. P. Paulikas, L. J. Nowicki, G. W. Crabtree, H. Claus, and W. K. Kwok, *Phys. Rev. B* **41,** 1863 (1990).
5. R. J. Cava, A. W. Hewat, E. A. Hewat, B. Batlogg, M. Marezio, K. M. Rabe, J. J. Krajewski, W. F. Peck Jr., and L. W. Rupp Jr., *Physica C* **165,** 419 (1990).
6. C. Greaves and P. R. Slater, *Supercond. Sci. Technol.* **2,** 5 (1989).
7. E. M. McCarron, M. K. Crawford, and J. B. Parise, *J. Solid State Chem.* **78,** 192 (1989).
8. V. P. S. Awana, S. K. Malik, and W. B. Yelon, *Physica C* **262,** 272 (1996).
9. H. Casalta, H. Alloul, and J.-F. Marucco, *Physica C* **204,** 331 (1993).

10. D. P. Norton, D. H. Lowndes, B. C. Sales, J. D. Budai, B. C. Chakoumakos, and H. R. Kerchner, *Phys. Rev. Lett.* **66,** 1537 (1991).
11. M.-H. Whangbo and C. C. Torardi, *Science* **249,** 1143 (1990).
12. J. L. Tallon and N. E. Flower, *Physica C* **204,** 237 (1993).
13. J. B. Torrance, Y. Tokura, A. I. Nazzal, A. Bezinge, T. C. Huang, and S. S. P. Parkin, *Phys. Rev. Lett.* **61,** 1127 (1988).
14. G. Xiao and N. S. Rebello, *Physica C* **211,** 433 (1993).
15. T. Watanabe, M. Fujiwara, and N. Suzuki, *Physica C* **252,** 100 (1995).
16. Y. Sun, G. Strasser, E. Gornik, W. Seidenbusch, and W. Rauch, *Physica C* **206,** 291 (1993).
17. I. R. Fischer, P. S. I. P. N. de Silva, J. W. Loram, J. L. Tallon, A. Carrington, and J. R. Cooper, *Physica C* **235–240,** 1497 (1994).
18. C. Legros-Glédel, J.-F. Marucco, E. Vincent, D. Favrot, B. Poumellec, B. Touzelin, M. Gupta, and H. Alloul, *Physica C* **175,** 279 (1991).
19. B. Fischer, J. Genossar, C. G. Kuper, L. Patlagan, G. M. Reisner, and A. Knizhnik, *Phys. Rev. B* **47,** 6054 (1993).
20. A. G. Kontos, R. Dupree, and Z. P. Han, *Physica C* **247,** 1 (1995).
21. A. J. Vega, M. K. Crawford, E. M. McCarron, and W. E. Farneth, *Phys. Rev. B* **40,** 8878 (1989).
22. W. I. F. David, RAL Report, Didcot, England, p. 88. 1988.
23. V. F. Sears, *Neutron News* **3,** 26 (1992).
24. M. Kakihana, M. Osada, M. Käll, L. Börjesson, H. Mazaki, H. Yasuoka, M. Yashima, and M. Yoshimura, *Phys. Rev. B* **53,** 11797 (1996).
25. J. L. Tallon, C. Bernhard, H. Shaked, R. L. Hitterman, and J. D. Jorgensen, *Phys. Rev. B* **51,** 12911 (1995).
26. I. D. Brown, *J. Solid State Chem.* **82,** 122 (1989).
27. I. D. Brown, *J. Solid State Chem.* **90,** 155 (1991).
28. J. L. Tallon, *Physica C* **168,** 85 (1990).
29. S.-G. Eriksson, C. Ström, P. Berastegui, M. Osada, M. Kakihana, M. Käll, and L. Börjesson, *Physica C* **235–240,** 389 (1994).
30. S.-G. Eriksson, C. Ström, M. Kakihana, Hj. Mattausch, and A. Simon, submitted for publication.
31. P. Fischer, E. Kaldis, J. Karpinski, S. Rusiecki, E. Jilek, V. Trounov, and A. W. Hewat, *Physica C* **205,** 259 (1993).